

# Dissipative Effects on Reheating after Inflation

Kyohei Mukaida<sup>(a)</sup> and Kazunori Nakayama<sup>(a,b)</sup>

<sup>a</sup>*Department of Physics, University of Tokyo, Bunkyo-ku, Tokyo 113-0033, Japan*

<sup>b</sup>*Kavli Institute for the Physics and Mathematics of the Universe, University of Tokyo,  
Kashiwa 277-8583, Japan*

## Abstract

The inflaton must convert its energy into radiation after inflation, which, in a conventional scenario, is caused by the perturbative inflaton decay. This reheating process would be much more complicated in some cases: the decay products obtain masses from an oscillating inflaton and thermal environment, and hence the conventional reheating scenario can be modified. We study in detail processes of particle production from the inflaton, their subsequent thermalization and evolution of inflaton/plasma system by taking dissipation of the inflaton in a hot plasma into account. It is shown that the reheating temperature is significantly affected by these effects.

# 1 Introduction

The idea of inflation [1, 2] has now become a part of standard cosmological evolution scenario. It provides beautiful explanations for the nearly flat isotropic/homogeneous Universe and the origin of primordial density fluctuation, which results in rich observed cosmological structures. For successful inflation, the energy of the inflaton, which drives the inflationary expansion of the Universe, must be transferred to the radiation consisting of hot standard model (SM) plasma. This process, called *reheating*, is rather an unknown aspect of inflation [3], partly because the process is model dependent and partly because the era of reheating is difficult to be explored observationally. However, the reheating temperature  $T_R$ , corresponding to the temperature of the hot plasma at the beginning of the radiation dominated era, is an important characteristics of inflation model since it often determines the efficiency of leptogenesis/baryogenesis and the abundance of (unwanted) relics such as the gravitino and moduli.

In a conventional picture, the inflaton is assumed to have a coupling to light fields and perturbatively decays into them. Produced light SM particles are thermalized and constitute radiation component of the Universe thereafter. In this case, the reheating temperature simply depends on the perturbative decay rate of the inflaton:

$$T_R^{(\text{w.b.})} \equiv \left( \frac{90}{\pi^2 g_*} \right)^{1/4} \sqrt{\Gamma_\phi^0 M_{\text{pl}}}, \quad (1.1)$$

where  $g_*$  is the relativistic degrees of freedom at the temperature  $T = T_R^{(\text{w.b.})}$ ,  $\Gamma_\phi^0$  denotes the inflaton decay rate evaluated at the vacuum and  $M_{\text{pl}}$  is the reduced Planck scale. Here we defined this quantity,  $T_R^{(\text{w.b.})}$ , as “would-be-reheating temperature”.

However, this simple picture does not hold for some inflation models for the following reasons. First, the inflaton is oscillating around its potential minimum, and hence masses of coupled particles also oscillate with time, which would invalidate the use of the inflaton decay rate at the vacuum [4, 5, 6]. Second, before the complete decay of the inflaton, the Universe is often already filled with high-temperature plasma. Thus light particles, including SM particles, obtain thermal masses and should be treated as quasi-particles, which would significantly modify the inflaton decay rate into these particles. On this second aspect, it was pointed out that large thermal masses of decay products prevent the inflaton decay and the temperature of plasma cannot be as high as the inflaton mass (divided by a coupling constant) [7]. This is not true: in high-temperature environment, the quasi-particles obtain thermal widths and the inflaton dissipates its energy into thermal plasma as was explicitly shown in Refs. [8, 9] in the context of reheating. Intuitively this is understood as a result of efficient scattering processes between inflaton and quasi-particles in thermal plasma. Thus actual thermal history would be much more complicated and, in particular, the reheating temperature would be significantly different from the estimate (1.1).

In this paper we address the issues of thermalization and reheating after inflation in detail. We start from the inflaton oscillation just after inflation and show how particle

production and their thermalization occur. Then we study the evolution of the inflaton oscillation and plasma by taking into account the inflaton dissipation in high-temperature plasma and also the non-perturbative particle production, until the inflaton dissipates all its energy, after which the radiation dominated Universe begins. Formulations for these effects are found in our previous paper [10], where dynamics of scalar fields in thermal environment was studied in detail.

It is shown that deviation from the conventional reheating scenario becomes more prominent for smaller inflaton mass, and hence we mainly focus on low-scale inflation model. Such low scale inflation is actually realized in the Higgs inflation [11, 12], where the SM Higgs field plays a role of inflaton, since its mass around the vacuum is weak scale. Some supersymmetric (SUSY) inflation models are also classified into this category: *e.g.*, MSSM inflation [13], alchemical inflation [14] or others.

In Sec. 2, we briefly discuss particle production and their thermalization. Dissipation coefficients in thermal plasma are also listed. Using these ingredients, we study the evolution of inflaton and plasma system, and determine the reheating temperature in Sec. 3. We conclude in Sec. 4.

## 2 Particle production and dissipation

### 2.1 Setup

Let us consider a following simple setup where the inflaton  $\phi$  interacts with light fields  $\chi$  via Yukawa interaction:

$$\mathcal{L} = \mathcal{L}_{\text{kin}} - \frac{1}{2}m_\phi^2\phi^2 + \lambda\phi(\bar{\chi}_L\chi_R + \text{h.c.}) + \mathcal{L}_{\text{other}} \quad (2.1)$$

where  $\lambda$  is a coupling constant taken to be real and positive,  $\mathcal{L}_{\text{kin}}$  denotes canonical kinetic terms, and  $\mathcal{L}_{\text{other}}$  denotes the other light degrees of freedom including gauge bosons. The bare mass of  $\chi$  is neglected in what follows. We also assume that the  $\chi$  fields are charged under some gauge groups and they interact with other light degrees of freedom via these gauge interactions. The coupling constant  $\lambda$  and gauge coupling  $g$  are assumed to be smaller than unity.<sup>#1</sup> We also define  $\alpha \equiv g^2/(4\pi)$  for later convenience.

Note that the model (2.1) should be regarded as a representative model which correctly describes essential features of more general class of models. It is straightforward to extend the model as

$$\mathcal{L} = \mathcal{L}_{\text{kin}} - \sum_{k,l} \frac{1}{2}m_{\phi_{kl}}^2\phi_{kl}^2 + \sum_{k,l} \lambda_{kl}\phi_{kl}(\bar{\chi}_{L,k}\chi_{R,l} + \text{h.c.}) + \mathcal{L}_{\text{other}}, \quad (2.2)$$

---

<sup>#1</sup> It is possible to consider the case where Yukawa interactions dominantly connect the  $\chi$  fields with the other light degrees of freedom. The following calculation does not change much if the coupling constant  $g$  is reinterpreted as the Yukawa coupling.

where integers  $k, l$  include possible flavor and gauge indices. In particular, the inflaton can have gauge charges. If one of the scalar fields  $\phi_{kl}$  obtains a large field value and takes a role of inflaton, the dynamics of inflaton is effectively described by a simplified model (2.1). In a SUSY model, there should be a inflaton coupling to bosons as  $\mathcal{L} = \lambda^2 |\phi|^2 |\tilde{\chi}|^2$  with  $\tilde{\chi}$  denoting the scalar partner of  $\chi$ . Inclusion of this coupling does not modify the following arguments, as long as we restrict ourselves to the case where the parametric resonant phenomena do not occur (see Sec. 2.2).

The initial amplitude of inflaton at the end of inflation,  $\phi_i$ , is taken as a free parameter, without specifying the inflaton potential beyond  $\phi_i$ . We only assume that the subsequent coherent oscillation can be well described by the quadratic potential:  $m_\phi^2 \phi^2/2$ . As mentioned in the Introduction, for the small amplitude case, *i.e.*  $m_\phi \gg \lambda \tilde{\phi}$  with  $\tilde{\phi}$  representing the amplitude of oscillating inflaton field,<sup>#2</sup> the effect of thermal plasma on the inflaton dissipation was already studied by [8, 9]. Hence, hereafter, we mainly concentrate on the large amplitude case:  $m_\phi \ll \lambda \tilde{\phi}$ . The purpose of this paper is to clarify the thermalization and reheating process in this class of models, especially the reheating temperature, by solving the evolution of inflaton and plasma system.

The basic ingredients that we will use in the following discussion are found in detail in our previous paper [10] and here we briefly repeat the results. Let us see what happens after inflation in the following subsections.

## 2.2 Particle production and thermalization

### 2.2.1 Instant preheating

After the inflation, the inflaton starts to oscillate around its potential minimum with an initial amplitude  $\phi_i$ . Hence, the coupled field  $\chi$  has an amplitude-dependent dispersion relation:  $\omega_\chi^2 = k^2 + m_{\text{th}}^\chi(T)^2 + \lambda^2 \phi^2(t)$  where  $m_{\text{th}}^\chi(T)$  denotes a possible thermal mass. Initially the thermal mass vanishes ( $m_{\text{th}}^\chi = 0$ ), since there is no background plasma. If  $\lambda \phi_i \ll m_\phi$ , the perturbative decay of the inflaton into  $\chi$  creates thermal plasma as in a conventional scenario. On the other hand, if  $\lambda \phi_i \gg m_\phi$ , such a process is kinematically blocked due to the  $\phi$ -dependent mass of  $\chi$  at the most time domains in each one oscillation of the inflaton. Instead, the following non-perturbative particle production process becomes important.<sup>#3</sup>

The efficient non-perturbative particle production occurs when the adiabaticity of the coupled  $\chi$  fields is broken down [4]:  $|\dot{\omega}_\chi/\omega_\chi^2| \gg 1$ . From this inequality, the following condition is obtained:

$$\lambda \tilde{\phi} \gg \max \left[ m_\phi, \frac{g^2 T^2}{m_\phi} \right]. \quad (2.3)$$

---

<sup>#2</sup>  $\tilde{\phi}$  and  $\phi(t)$  represent the amplitude and oscillating field value respectively.

<sup>#3</sup> The perturbative inflaton decay into gauge bosons through one-loop process involving  $\chi$  field is possible, but its efficiency is lower than that of the non-perturbative particle production.

Here  $\tilde{\phi}$  stands for the amplitude of  $\phi$ . Importantly, Eq. (2.3) implies that if the thermal mass  $m_{\text{th}}^\chi(T) \sim gT$  becomes as large as  $k_* \equiv (\lambda\tilde{\phi}m_\phi)^{1/2}$ , then the non-perturbative particle production does not occur [10]. If Eq. (2.3) is met, the  $\chi$ 's modes below the typical momentum  $k_*$  are amplified in each oscillation, and the typical number density for one degree of freedom can be evaluated as

$$n_\chi \sim \frac{k_*^3}{(2\pi)^3} \sim \frac{(\lambda\tilde{\phi}m_\phi)^{3/2}}{8\pi^3}; \quad (2.4)$$

in each oscillation.

After the  $\phi$  passes through the origin, the produced particles become heavy due to the field value of oscillating  $\phi$ , and their decay rate becomes large correspondingly. If the decay rate of  $\chi$ :  $\Gamma_\chi$  is sufficiently large, they eventually decay into the other light degrees of freedom at  $\Gamma_\chi(\phi(t_{\text{dec}})) t_{\text{dec}} \sim 1$  well before the  $\phi$  reaches its maximum value [6]. This is the case for  $m_\phi \ll \alpha\lambda\tilde{\phi}$ , if we assume that the typical decay rate of  $\chi$  is given by  $\Gamma_\chi \sim \alpha m_\chi \sim \alpha\lambda|\phi(t)|$ . In this case, a linear potential for  $\phi$  generated by the produced particles [4] is insignificant, since the produced particles decay when the inflaton field value reaches  $\phi \sim [m_\phi\tilde{\phi}/(\alpha\lambda)]^{1/2} \ll \tilde{\phi}$ .

In addition, if the inflaton couples to the bosonic fields  $\tilde{\chi}$ , this condition guarantees the absence of violent parametric resonant phenomena. Unless the coupled bosonic particles decay before the inflaton moves back to the origin, the production rate of these bosonic particles is enhanced due to the induced emission effect. Thus, their number density grows exponentially whenever the inflaton passes through the origin, and as a result, the system may enter the so-called turbulent regime as shown in Refs. [15] with classical lattice simulations and recently in Refs. [16] with Kadanoff-Baym eqs.

Throughout this paper, we assume that the condition  $m_\phi \ll \alpha\lambda\tilde{\phi}$  holds, and hence such effects can be neglected.<sup>#4</sup> The energy density converted to the other light degrees of freedom in one inflaton oscillation can be evaluated as

$$\delta\rho \sim m_\chi n_\chi|_{\text{dec}} \sim \alpha^{-1/2}(\lambda\tilde{\phi}m_\phi)^2. \quad (2.5)$$

### 2.2.2 Thermalization of plasma

In order to study the subsequent evolution of the produced plasma and oscillating scalar field  $\phi$  at every moment, it is practically important to know whether or not the produced other light degrees of freedom can attain thermal equilibrium in a time scale faster than the oscillation time scale of  $\phi$  [17].

At the first passage of  $\phi \sim 0$ , the total energy density of light degrees of freedom  $\rho_{\text{rad}}$  is given by  $\rho_{\text{rad}} = \delta\rho$ , since there are no particles before this non-perturbative particle

---

<sup>#4</sup> The number density of particles produced by the decay of  $\chi$  fields directly coupled to the inflaton cannot become so large since otherwise the non-perturbative production becomes inactive due to the large screening mass:  $m_s \gtrsim k_*$  [cf. Eq. (2.3)].

production. In this case, as extensively discussed in Ref. [18], the thermalization time scale of light degrees is estimated by

$$t_{\text{eq}} \sim (\alpha^2 T_{\text{f}})^{-1} \sqrt{Q/T_{\text{f}}} \sim \alpha^{-33/16} (\lambda \tilde{\phi} m_{\phi})^{-1/2}, \quad (2.6)$$

where  $T_{\text{f}} \sim \rho_{\text{rad}}^{1/4}$  and the typical momentum scale  $Q$  is given by  $Q \sim m_{\chi}|_{\text{dec}} \sim \alpha^{-1/2} (\lambda \tilde{\phi} m_{\phi})^{1/2}$ . [See Appendix A for more detail.] Therefore, the produced other light degrees of freedom can be safely regarded as “thermal” plasma as far as the following condition is met:

$$1 \ll \alpha^{33/16} (\lambda \tilde{\phi} / m_{\phi})^{1/2}. \quad (2.7)$$

As one can see, this condition is satisfied if the initial amplitude of oscillating scalar field  $\phi_i$  is sufficiently large.

After several oscillations, the energy density of background thermal plasma becomes much larger than the one produced via the non-perturbative production in each oscillation, *i.e.*  $\rho_{\text{rad}} \gg \delta\rho$ . In this case, the equilibration time is given by the relaxation one, corresponding to a time scale for a hard particle  $Q > T$  to emit its energy away to the thermal plasma of temperature  $T$ :<sup>#5</sup>

$$t_{\text{rlx}} \sim (\alpha^2 T)^{-1} \sqrt{Q/T}. \quad (2.8)$$

Hence, the background plasma can remain in thermal equilibrium if  $t_{\text{rlx}} \ll m_{\phi}^{-1}$ .

If these conditions are met, the produced light particles attain thermal equilibrium in each oscillation, and consequently the screening mass of coupled  $\chi$  field can be described by the thermal mass  $m_{\chi} \sim gT$ .<sup>#6</sup> As mentioned above [Eq. (2.3)], the instant preheating stage finishes when this thermal mass becomes comparable to  $k_* \sim (\lambda \tilde{\phi} m_{\phi})^{1/2}$ .

## 2.3 Dissipation to thermal plasma

As discussed in the previous subsection, the background thermal plasma is produced via the instant preheating if  $\lambda\phi_i > m_{\phi}$ , just after inflation. The produced thermal plasma can significantly affect subsequent dynamics of oscillating inflaton field. Aside from the blocking effect on the non-perturbative production due to the thermal mass, which we discussed in the previous section, there are basically two effects from thermal environment: (i) thermal effective potential for the inflaton and (ii) dissipation of the inflaton to thermal plasma. We are mainly interested in the situation where the scalar field dominates the Universe, and hence let us discuss the latter effect (ii).<sup>#7</sup>

---

<sup>#5</sup> Note that this temperature  $T$  is not related to the  $Q$ , contrary to the  $T_{\text{f}}$ .

<sup>#6</sup> Otherwise, the effective mass for  $\chi$  cannot be described by a temperature  $T$  and following analyses become more complicated. We do not go into such a case in this paper.

<sup>#7</sup> If the scalar field  $\phi$  oscillates dominantly with the thermal potential (*e.g.* thermal mass or thermal log), its energy density is bounded as  $\rho_{\phi} \lesssim T^4$  [10]. Therefore, it is typically less than the energy density of thermal plasma:  $\rho_{\text{rad}} \sim g_* T^4 > \rho_{\phi}$ .

We will not perform detailed calculations of the dissipation coefficient and will not show all the list of dissipation coefficients in various regimes in this section. Instead, let us explain its typical behavior and intuitive physical interpretation relevant to our following discussion. We refer to Refs. [9, 10, 19, 20] for basic formalism to calculate them. The complete list of dissipation coefficient in various regimes is summarized in Appendix B.

The effect of thermal plasma becomes significant in the case where the typical time scale of oscillation is much slower than that of interaction in thermal plasma, *i.e.*  $m_\phi \ll \alpha T$ . In this case, the oscillating scalar field  $\phi$  cannot decay into light degrees of freedom, since these would-be decay products acquire thermal masses which are larger than the  $\phi$  mass. However, the oscillating scalar can dissipate into thermal plasma through multiple scattering by light particles in thermal plasma, or more precisely through thermal width of each quasi-particle excitation.

The dissipation coefficient depends on the value of  $\phi$ , and its dependence can be divided into two regimes: (i) small field value regime  $\lambda\phi \ll T$  and (ii) large field value regime  $\lambda\phi \gg T$ . In the case (i), the coupled  $\chi$  particles are relativistic and its number density is given by  $T^3$ . Hence, the oscillating scalar dissipates its energy through scatterings involving  $\chi$  particles. On the other hand, in the case (ii), such processes are unlikely to occur since the  $\chi$  particles become very heavy due to the amplitude of  $\phi$  and the number density of  $\chi$  is exponentially suppressed correspondingly. Therefore, the oscillating scalar dissipates its energy mainly by multiple scattering of gauge bosons through a higher dimensional operator obtained from integrating out the heavy  $\chi$  field. Consequently, the dissipation coefficient for  $m_\phi \ll \alpha T$  can be evaluated as [10]

$$\Gamma_\phi \sim \begin{cases} A_0 \dim(r) \lambda^2 \alpha T / (2\pi^2) & \text{for } \lambda\phi \ll m_{\text{th}}^\chi \sim gT \\ A_0 \dim(r) \lambda^4 \phi^2 / (\pi^2 \alpha T) & \text{for } m_{\text{th}}^\chi \sim gT \ll \lambda\phi \ll T \\ b \alpha^2 T^3 / \phi^2 & \text{for } \lambda\phi \gg T \end{cases} \quad (2.9)$$

where

$$b := \left( \frac{T(r)}{16\pi^2} \right)^2 \frac{(12\pi)^2}{\ln \alpha^{-1}}. \quad (2.10)$$

Here  $\dim(r)$  stands for the dimension of  $\chi$ 's representation  $r$  of gauge group and  $T(r)$  is the index of  $\chi$ 's representation  $r$  defined by  $T(r)\delta^{ab} = \text{tr}[t^a(r)t^b(r)]$ , and  $A_0$  is a numerical constant, typically  $A_0 \sim 1/2$ . For our numerical calculation, we take  $\alpha = 0.05$ , and then it is given by  $A_0 \simeq 0.3$ . Note that the above dissipative coefficient is calculated in two limits: large and small amplitude, and hence we have some ambiguities in the intermediate regime.<sup>#8</sup>

In the opposite limit,  $m_\phi > T$ , the dissipation coefficient can be estimated with neglecting the finite density correction to the dispersion relation of  $\chi$ . Therefore, it is simply

---

<sup>#8</sup> In addition, the small amplitude result computed with one-loop approximation may change by some factors due to the resummation of infinitely many higher-loop diagrams as discussed in Ref. [20].

given by the perturbative decay rate of oscillating scalar into light degrees of freedom. If the amplitude  $\tilde{\phi}$  is much larger than the mass of  $\phi$  (*i.e.*  $\lambda\tilde{\phi} \gg m_\phi$ ), the oscillating scalar  $\phi$  loses its energy mainly via the non-perturbative particle production as discussed in the previous section. Hence, practically, the perturbative decay becomes important at  $\lambda\tilde{\phi} \ll m_\phi$  and it is given by

$$\Gamma_\phi = \text{dim}(r) \frac{\lambda^2 m_\phi}{8\pi}. \quad (2.11)$$

In the intermediate region:  $\alpha T \lesssim m_\phi \lesssim gT$ , the perturbative decay is kinematically suppressed due to thermal masses of quasi-particles, and a non-zero dissipation rate comes from their thermal widths [8, 9]. As a result, the dissipation coefficient can be approximately expressed as

$$\Gamma_\phi \simeq \text{dim}(r) \begin{cases} \frac{\lambda^2 m_\phi}{8\pi} \sqrt{1 - 4 \frac{m_{\text{th}}^{\chi^2}}{m_\phi^2}} [1 - 2f_{\text{FD}}(m_\phi/2)] & \text{for } m_\phi > 2m_{\text{th}}^\chi \\ \frac{\lambda^2 \alpha T}{2\pi^2} \left( A_0 + A_1 \left[ \frac{m_\phi}{\alpha T} \right]^2 + \dots \right) & \text{for } 2m_{\text{th}}^\chi < m_\phi, \end{cases} \quad (2.12)$$

where  $f_{\text{FD}}$  denotes the Fermi-Dirac distribution.  $A_0$  and  $A_1$  are numerical constants, and in our numerical computation with  $\alpha = 0.05$ , they are given by  $A_0 \simeq 0.3$  and  $A_1 \simeq 2 \times 10^{-4}$  respectively. Note that this result is applicable to all the  $m_\phi$  region in a small amplitude regime:  $\lambda\tilde{\phi} < m_{\text{th}}^\chi \sim gT$ .

### 3 Reheating after inflation

In the last two subsections, we have introduced basic ingredients to study the dynamics of oscillating inflaton. In this section, let us study the dynamics of oscillating inflaton and numerically evaluate the reheating temperature with some examples.

#### 3.1 Effective dissipation rate of the inflaton

The equation of motion of the inflaton is given by

$$\ddot{\phi} + (3H + \Gamma_\phi)\dot{\phi} + m_\phi^2 \phi = 0, \quad (3.1)$$

where  $\Gamma_\phi$  is the  $\phi$ -dependent dissipation coefficient and  $H$  is the Hubble parameter. In order to study the dynamics of oscillating scalar field, it is convenient to consider quantities averaged over a time interval that is longer than the oscillation time scale but shorter than the Hubble and dissipation time scale. Taking this time average, one finds

$$\dot{\rho}_\phi + 3H\rho_\phi = -\Gamma_\phi^{\text{eff}} \rho_\phi, \quad (3.2)$$

$$\dot{\rho}_{\text{rad}} + 4H\rho_{\text{rad}} = \Gamma_\phi^{\text{eff}} \rho_\phi, \quad (3.3)$$

$$3M_{\text{pl}}^2 H^2 = \rho_\phi + \rho_{\text{rad}}, \quad (3.4)$$



where  $M_{\text{pl}}$  is the reduced Planck mass,  $\rho_{\text{rad}}$  stands for the energy density of radiation, the energy density of inflaton is given by  $\rho_\phi := \overline{\dot{\phi}^2/2 + m_\phi^2 \phi^2/2}$  and the effective dissipation rate is defined as  $\Gamma_\phi^{\text{eff}} := \overline{\Gamma_\phi \dot{\phi}^2 / \dot{\phi}^2}$ . Here the time-averaged quantity is represented by  $\overline{\cdots}$ . Since  $\Gamma_\phi$  depends on  $\phi$ ,  $\Gamma_\phi^{\text{eff}}$  is different from  $\Gamma_\phi$  in general. Let us summarize the effective dissipation rate  $\Gamma_\phi^{\text{eff}}$  relevant to our following discussion. The complete list is shown in Appendix B.

The effective dissipation coefficient is independent of the amplitude  $\tilde{\phi}$  in the small amplitude regime ( $\lambda\tilde{\phi} \lesssim m_{\text{th}}^\chi \sim gT$ ) [See Eq. (B.6)]:

$$\Gamma_\phi^{\text{eff}} \simeq \text{dim}(r) \begin{cases} \frac{\lambda^2 m_\phi}{8\pi} \sqrt{1 - 4 \frac{m_{\text{th}}^{\chi 2}}{m_\phi^2}} [1 - 2f_{\text{FD}}(m_\phi/2)] & \text{for } 2m_{\text{th}}^\chi < m_\phi \\ \frac{\lambda^2 \alpha T}{2\pi^2} \left( A_0 + A_1 \left[ \frac{m_\phi}{\alpha T} \right]^2 \right) & \text{for } m_\phi < 2m_{\text{th}}^\chi. \end{cases} \quad (3.5)$$

For our numerical computation, we take  $\alpha = 0.05$ , and then the numerical constants  $A_0$  and  $A_1$  are given by  $A_0 \simeq 0.3$  and  $A_1 \simeq 2 \times 10^{-4}$  respectively. The effective dissipation rate for non-perturbative production is also independent of  $\tilde{\phi}$  and it is given by

$$\Gamma_\phi^{\text{eff}}|_{\text{NP}} = \text{dim}(r) \frac{\lambda^2 m_\phi}{\pi^4 \sqrt{\alpha}} \text{ for } \lambda\tilde{\phi} \gg \max \left[ m_\phi, \frac{g^2 T^2}{m_\phi} \right]. \quad (3.6)$$

On the other hand, if the amplitude  $\tilde{\phi}$  is larger than  $m_{\text{th}}^\chi$ , then the effective dissipation coefficient depends on  $\tilde{\phi}$ . In particular, the effective dissipation coefficient for the regime  $m_\phi < \alpha T$  is important in the following discussion. In this case, the effective dissipation coefficient can be approximated as [Eq. (B.16)]

$$\Gamma_\phi^{\text{eff}} \simeq C \frac{4}{3\pi^3} \tilde{A}_0 \text{dim}(r) \frac{\lambda T^2}{\alpha \tilde{\phi}} \text{ for } \lambda\tilde{\phi} \gg T. \quad (3.7)$$

Here we have explicitly included an uncertainty in a numerical constant  $C$  that is caused by the extrapolation in the intermediate regime as we already mentioned, and it is taken to be unity:  $C = 1$  for our numerical computation. Practically, the dissipation coefficient for  $m_{\text{th}}^\chi < \lambda\tilde{\phi} < T$  is not important, since this term  $\Gamma_\phi^{\text{eff}} \propto \tilde{\phi}^2$  [See Eq. (B.19)] cannot complete the reheating of the Universe because it decreases faster than the Hubble parameter. [See also Fig. 1 and footnote #9.]

### 3.2 Evolution of inflaton/plasma system and reheating

Now we are in a position to calculate the evolution of inflaton/plasma system after inflation. We numerically solve the differential Eqs. (3.2) – (3.4) to study the dynamics

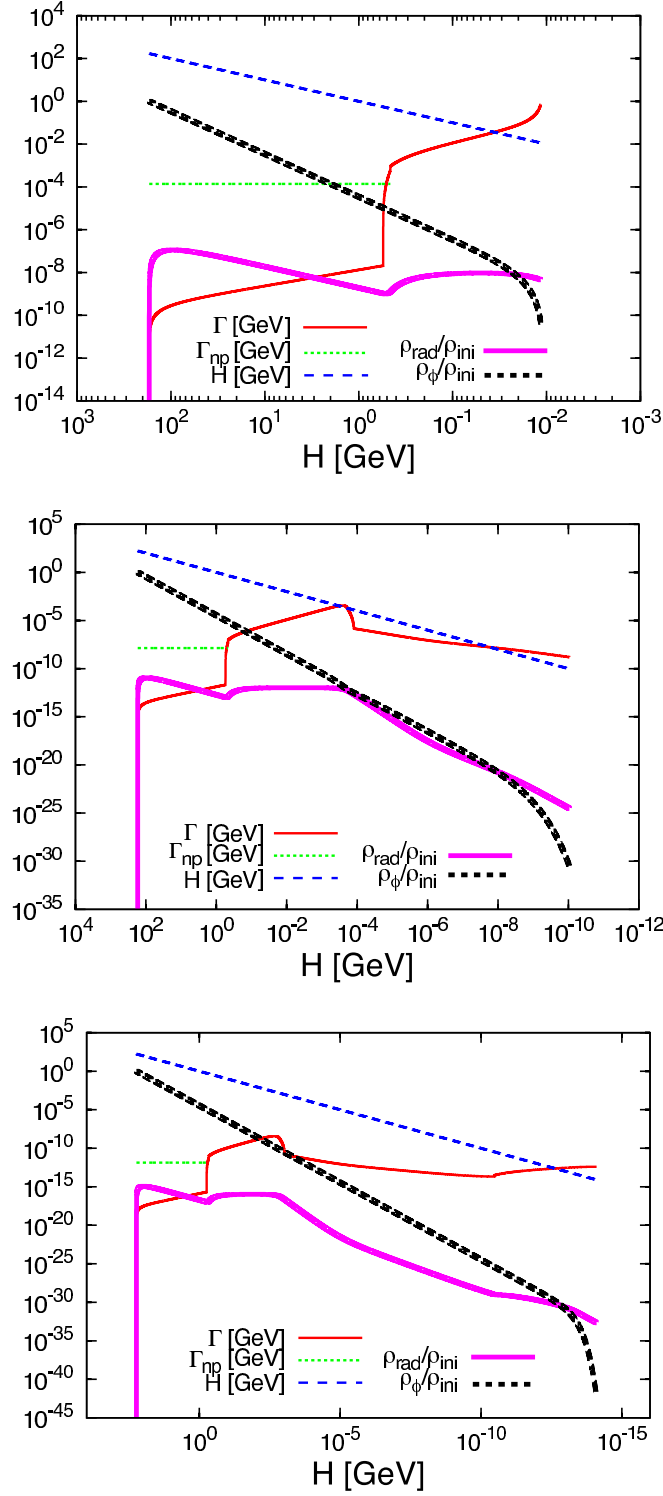


Figure 1: The evolution of various quantities as a function of Hubble scale  $H$ : the effective dissipation rate except for non-perturbative particle production  $\Gamma$  (*red thin solid*), one for non-perturbative particle production  $\Gamma_{\text{np}}$  (*green thin dotted*), the energy density of radiation  $\rho_{\text{rad}}$  (*magenta thick solid*) and inflaton  $\rho_{\phi}$  (*black thick dashed*) normalized by an initial energy density  $\rho_{\text{ini}}$ . **Top:**  $(m_{\phi}, \lambda, \phi_i) = (1 \text{ TeV}, 10^{-3}, 10^{18} \text{ GeV})$ , **Middle:**  $(m_{\phi}, \lambda, \phi_i) = (1 \text{ TeV}, 10^{-5}, 10^{18} \text{ GeV})$ , **Bottom:**  $(m_{\phi}, \lambda, \phi_i) = (1 \text{ TeV}, 10^{-7}, 10^{18} \text{ GeV})$ .

of inflaton/plasma system, using the effective dissipation rate summarized in App. B.2. To make our discussion concrete, let us assume that  $\chi$  is an extra quark like matter charged under SU(3) with the fundamental representation in the following. Then, we have  $\dim(3) = 3$  and  $T(3) = 1/2$ . And the gauge coupling constant is assumed to be  $\alpha = 0.05$  hereafter.

Fig. 1 shows the evolution of various quantities as a function of Hubble scale  $H$ : the effective dissipation rate  $\Gamma_\phi^{\text{eff}}$  except for non-perturbative particle production, that for non-perturbative particle production  $\Gamma_\phi^{\text{eff}}|_{\text{NP}}$ , the energy density of radiation  $\rho_{\text{rad}}$  and inflaton  $\rho_\phi$ , normalized by an initial energy density  $\rho_{\text{ini}} (= m_\phi^2 \phi_i^2 / 2)$ .

The top panel is computed with  $(m_\phi, \lambda, \phi_i) = (1 \text{ TeV}, 10^{-3}, 10^{18} \text{ GeV})$ . First, the radiation with high temperature ( $T \sim 10^8 \text{ GeV}$ ) is produced via the instant preheating. The condition for non-perturbative production [Eq. (2.3)] soon saturates, since the amplitude scales as  $\tilde{\phi} \propto a^{-3/2}$  where  $a$  is the scale factor of the Universe while the temperature scales as  $T \propto a^{-3/8}$ , and consequently the non-perturbative production shuts off. Then, as can be seen from the plateau of  $\rho_{\text{rad}}$  around  $H \sim 5 \times 10^{-1} - 10^{-2} \text{ GeV}$ , the temperature of thermal plasma becomes nearly constant during the regime where the dominant dissipation rate is given by  $\Gamma_\phi^{\text{eff}} \sim \lambda T^2 / (\alpha \tilde{\phi})$ . At this regime, the energy density of radiation behaves as  $\rho_{\text{rad}} \sim \Gamma_\phi^{\text{eff}} \rho_\phi / H \sim M_{\text{pl}}^2 T^2 (H / \tilde{\phi})$ . Therefore, the temperature becomes constant since the inflaton dominates the Universe at that time. Finally, the reheating is completed at  $\Gamma_\phi^{\text{eff}} \sim H$ . In the top panel, the reheating takes place via  $\Gamma_\phi^{\text{eff}} \sim \lambda T^2 / (\alpha \tilde{\phi})$  at  $H \sim 2 \times 10^{-2} \text{ GeV}$ , and the reheating temperature is  $T_R \sim 10^8 \text{ GeV}$ .

The middle [bottom] panel is computed with  $(m_\phi, \lambda, \phi_i) = (1 \text{ TeV}, 10^{-5}, 10^{18} \text{ GeV})$  [ $(m_\phi, \lambda, \phi_i) = (1 \text{ TeV}, 10^{-7}, 10^{18} \text{ GeV})$ ]. The subsequent evolution is the same as the top panel case in the both middle and bottom panels. First, the thermal plasma is produced via the instant preheating, and the condition for non-perturbative production soon saturates. Then, the plateau region follows  $H \sim 5 \times 10^{-1} - 10^{-4} \text{ GeV}$  [ $H \sim 5 \times 10^{-1} - 10^{-3} \text{ GeV}$ ]. After that, since  $\tilde{\phi}$  decreases due to the cosmic expansion, the dominant dissipation rate becomes  $\Gamma_\phi^{\text{eff}} \sim \lambda^2 \alpha T$ . In the middle panel, the reheating takes place via  $\Gamma_\phi^{\text{eff}} \sim \lambda^2 \alpha T$  at  $H \sim 10^{-8} \text{ GeV}$ , and the reheating temperature is  $T_R \sim 10^5 \text{ GeV}$ . On the other hand, in the bottom panel, the reheating occurs via  $\Gamma_\phi^{\text{eff}} \sim \lambda^2 m_\phi$  at  $H \sim 10^{-13} \text{ GeV}$ , and its temperature is given by  $T_R \sim 3 \times 10^2 \text{ GeV}$ .<sup>#9</sup>

Analytically, the reheating temperature can be roughly estimated as follows in the

---

<sup>#9</sup> Usually, the reheating temperature  $T_R$  is defined as the temperature at which the radiation dominated Universe begins and it roughly corresponds to the epoch  $H \sim \Gamma_\phi$  as (1.1). In the present situation with thermal dissipation effect, this definition is ambiguous because of the peculiar behavior of  $\Gamma_\phi^{\text{eff}}$ . As seen in the middle panel of Fig. 1,  $\Gamma_\phi^{\text{eff}}$  can once become equal to  $H$  but the relation  $\rho_{\text{rad}} \sim \rho_\phi$  may hold thereafter without exponential decay of the inflaton for a while. This is because the dissipation rate decreases faster than the Hubble parameter during the regime:  $\Gamma_\phi^{\text{eff}} \propto \tilde{\phi}^2$ . Therefore, the reheating temperature  $T_R$  here is defined as the temperature at which the inflaton energy density begins to decrease exponentially. One should note that, although the parameter  $T_R$  is a convenient quantity which describes a global picture of the early Universe, actual thermal history before the reheating would be significantly different from a conventional one.

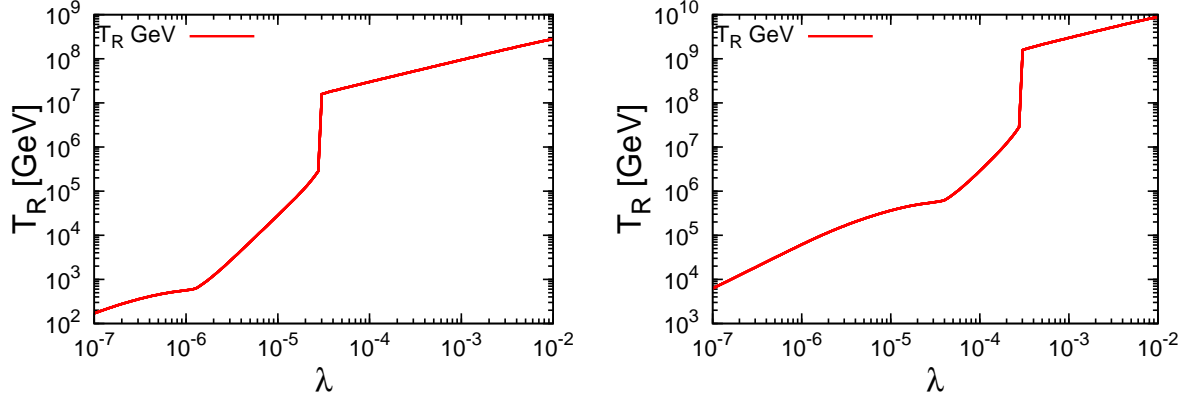


Figure 2: The reheating temperature  $T_R$  as a function of  $\lambda$  is shown. **Left:**  $m_\phi = 1$  TeV and **Right:**  $m_\phi = 10^3$  TeV.

three cases: reheating via (i)  $\Gamma_\phi^{\text{eff}} \sim \lambda T^2/(\alpha\tilde{\phi})$ , (ii)  $\Gamma_\phi^{\text{eff}} \sim \lambda^2\alpha T$  and (iii)  $\Gamma_\phi^{\text{eff}} \sim \lambda^2 m_\phi$  :

$$T_R \sim \begin{cases} C^{1/2} \left( \frac{\tilde{A}_0 \dim(r)}{g_* \alpha} \right)^{1/2} (\lambda M_{\text{pl}} m_\phi)^{1/2} & \dots \text{(i)} \\ \left( \frac{A_0^2 \dim(r)^2 \alpha^2}{g_*} \right)^{1/2} (\lambda^2 M_{\text{pl}}) & \dots \text{(ii)} \\ \left( \frac{\dim(r)}{g_*^{1/2}} \right)^{1/2} (\lambda^2 M_{\text{pl}} m_\phi)^{1/2} & \dots \text{(iii)} \end{cases} \quad (3.8)$$

Note that the resultant reheating temperature contains the uncertainty  $C$  from Eq. (3.7). Importantly, the coupling  $\lambda$  dependence differs among (i) – (iii) and the initial amplitude  $\phi_i$  dependence is absent even in the case (i). These behavior can be seen in Figs. 2 and 3. In Fig. 2, reheating temperature is plotted as a function of  $\lambda$  for  $m_\phi = 1$  TeV (left) and  $m_\phi = 10^3$  TeV (right) with  $\phi_i = 10^{18}$  GeV. It is seen that in the small  $\lambda$  limit, the reheating temperature is determined by the standard perturbative decay scenario (case (iii)). As  $T_R$  increases and approaches to  $m_\phi$  for larger  $\lambda$ , it begins to saturate due to the effect of thermal blocking. For larger  $\lambda$ , however, thermal dissipation comes in and again  $T_R$  increases [case (ii) and (i)]. This figure does not depend on  $\phi_i$  for  $\phi_i \gtrsim 10^{15}$  GeV. In Fig. 3, contours of reheating temperature as a function of  $\lambda$  and  $m_\phi$  are shown.

As mentioned in footnote #9, the reheating temperature  $T_R$  here is defined as the temperature at which the inflaton energy density begins to decrease exponentially. The sharp discontinuity between two regimes [(i) and (ii)] seen in Fig. 2 is related to the definition of reheating temperature  $T_R$ . The reheating cannot be completed during the regime where the effective dissipation rate is given by  $\Gamma_\phi^{\text{eff}} \propto \tilde{\phi}^2$ , with the definition of reheating that we employed. This is clearly seen in the middle panel of Fig. 1 ( $\lambda = 10^{-5}$ ):

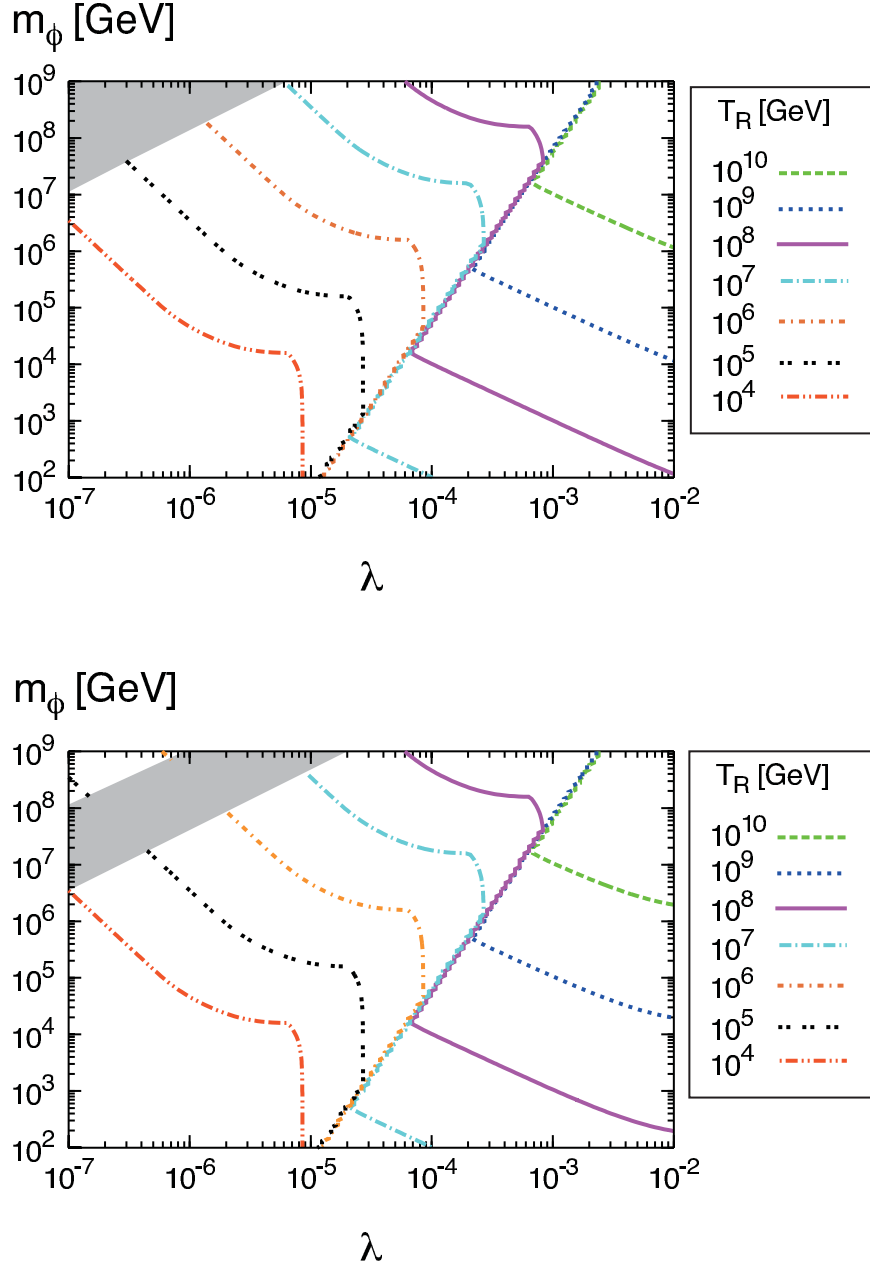


Figure 3: Contour plot of reheating temperature  $T_R$  as a function of  $\lambda$  and  $m_\phi$ ; **Top:**  $\phi_i = 10^{18}$  GeV and **Bottom:**  $\phi_i = 10^{15}$  GeV. Inside the shaded region, the condition  $\lambda \alpha \tilde{\phi} > m_\phi$  is violated, and this region depends on the initial amplitude  $\phi_i$ . At the upper left corner of bottom panel, one can see the region where the non-perturbative production is completely absent because  $\lambda \phi_i < m_\phi$ .

$\Gamma$  crosses  $H$  two times, but at the first crossing the reheating is not completed and the reheating temperature is roughly determined at the second crossing. For larger  $\lambda$ , the situation becomes close to the top panel of Fig. 1 ( $\lambda = 10^{-3}$ ), where reheating is completed soon after the first crossing. Thus the reheating temperature jumps somewhere around  $10^{-5} < \lambda < 10^{-3}$  (for  $m_\phi = 1$  TeV) if it is plotted as a function of  $\lambda$ . This is the reason for the behavior in Fig. 2.

Here we note that, for the purpose of estimating the reheating temperature, it is not necessary to impose the condition that the light degrees of freedom should be always kept in thermal equilibrium for every  $\phi$ 's oscillation. The only requirement is that the typical interaction time scale of plasma becomes much faster than the Hubble parameter and the dissipation rate of  $\phi$  before the reheating is completed.

## 4 Conclusions and Discussion

In this paper we have investigated the issue of reheating and thermalization after inflation. If the inflaton is not heavy enough and its coupling to light species is not so small, the standard reheating scenario in which the perturbative decay of the inflaton triggers the reheating may not hold. In such a case, we need to carefully study the particle production, thermalization, and the resulting dissipation effect on the inflaton coherent oscillation. Actually, we found that the dissipation effect in thermal plasma plays a crucial role in the completion of reheating, and the reheating temperature can be much higher than the inflaton mass. This is consistent with the statement of Refs. [8, 9], but our setup and methods are more general and have broad applicability to concrete models.

For example, in the Higgs inflation [11, 12] scenario (see Refs. [21, 22] for its realization in NMSSM), the inflaton mass around the vacuum is weak scale. Although  $\phi^4$  potential is dominant after inflation and the evolution of inflaton/plasma system would be different from our model, the final process of reheating cannot be understood without taking the dissipation effect into account, as studied in this paper. MSSM inflation [13] is another example in which the inflaton is very light. Non-perturbative particle production is expected at the first several oscillations [17], but the final reheating may be caused by dissipative effects in thermal plasma. Similar results may hold for alchemical inflation scenario [14], in which the inflaton has a mass of soft SUSY breaking scale and oscillates around the origin after inflation. It will also be useful for reheating after a class of thermal inflation model [23]. It should also be noticed that the evolution of thermal plasma before the complete reheating in these cases can significantly differ from a conventional scenario. Phenomenological consequences, such as relic abundance of heavy particles created in high-temperature plasma and the efficiency of baryogenesis, may not be characterized by a single parameter  $T_R$ , but by a detailed thermal history before reheating. We will further generalize our results and apply to concrete models in a separate paper.

If the inflaton oscillates around a large VEV as in the case of new inflation [2], it is expected that the dissipation effect would be much milder and the conventional reheating

scenario by the perturbative decay would be appropriate for broader parameter spaces. This might also be true in hybrid inflation [24, 25], although it is rather non-trivial because the inflaton oscillates around the origin while the waterfall field oscillates around a large VEV. We leave these issues for a future work.

Finally we comment on the fate of particle-like excitations of inflaton. In the case where thermal dissipation plays a crucial role for the reheating with  $T_R > m_\phi$ , the inflaton particles are expected to have (nearly) thermal abundance. When the temperature decreases to  $T \sim m_\phi/20$  after the completion of reheating, the inflaton freezes out from thermal bath. At this stage, the perturbative decay of the inflaton opens since the temperature is lower than the inflaton mass, and the decay rate is given by  $\sim \lambda^2 m_\phi$ , which is much larger than the Hubble rate at this epoch,  $H \sim 10^{-2} m_\phi^2/M_P$  unless  $\lambda$  is extremely small. Therefore, the inflaton particles decay into light species and disappear as soon as they freeze out from thermal bath.

## Acknowledgment

This work is supported by Grant-in-Aid for Scientific research from the Ministry of Education, Science, Sports, and Culture (MEXT), Japan, No. 21111006 (K.N.) and No. 22244030 (K.N.) and also by World Premier International Research Center Initiative (WPI Initiative), MEXT, Japan. The work of K.M. is supported in part by JSPS Research Fellowships for Young Scientists.

## A Thermalization

In this section, let us briefly review the thermalization of weakly coupled plasma for the case of instant preheating, following Ref. [18].

As discussed in Sec. 2.2, due to the break-down of adiabaticity of the coupled particles  $\chi$  around  $\phi \sim 0$ ,  $\chi$  particles are produced non-perturbatively in each oscillation as shown in Eq. (2.4). After the passage of origin  $\phi \sim 0$ , they become heavier and the decay rate becomes larger correspondingly. Eventually, they decay into the other light degrees of freedom at  $\Gamma_\chi(\phi(t_{\text{dec}}))t_{\text{dec}} \sim 1$  before the  $\phi$  comes back to the origin, if the decay rate of  $\chi$ , given by  $\Gamma_\chi$ , is sufficiently large. Assuming the typical decay rate of  $\chi$  as  $\Gamma_\chi \sim \theta^2 \alpha m_\chi \sim \theta^2 \alpha \lambda |\phi(t)|$ , one finds that this is the case for  $m_\phi \ll \theta^2 \alpha \lambda \tilde{\phi}$ . Here  $\theta$  denotes the mixing between  $\chi$  and other light degrees of freedom. In this case, energy density of the other light degrees of freedom is given by

$$\delta\rho \sim m_\chi n_\chi|_{\text{dec}} \sim \theta^{-1} \alpha^{-1/2} \lambda^2 m_\phi^2 \tilde{\phi}^2; \quad (\text{A.1})$$

in each oscillation. The typical momentum of decay products is roughly given by

$$Q \sim m_\chi|_{\text{dec}} \sim \theta^{-1} \alpha^{-1/2} \lambda^{1/2} m_\phi^{1/2} \tilde{\phi}^{1/2}. \quad (\text{A.2})$$

Therefore, the converted energy density can be expressed as

$$\delta\rho \sim \theta^3 \alpha^{3/2} Q^4. \quad (\text{A.3})$$

Hereafter, we assume that the mixing  $\theta$  is  $\mathcal{O}(1)$ . In fact, the size of mixing angle is not so important in the following discussion. [See footnote #11.]

At the first passage of  $\phi \sim 0$ , the total energy density of light degrees of freedom is estimated as  $\rho = \delta\rho \sim \alpha^{3/2} Q^4$ . This is the so-called under occupied case [18], since the momentum distribution  $f$  around the typical momentum  $Q$  can be evaluated as  $f(Q) \sim \alpha^{3/2} < 1$ . It is instructive to compare the typical momentum  $Q$  with the “temperature”, defined as  $T_f \sim \rho^{1/4}$ . This temperature can be expressed as  $T_f \sim \alpha^{3/8} Q$ , and hence it is smaller than  $Q$ . This means that the typical phase space distribution of produced particles for the first crossing of  $\phi \sim 0$  are concentrated on the UV regime, compared to the thermal equilibrium distribution. As discussed in [18], in this UV dominated case, the subsequent thermalization takes place as follows.<sup>#10</sup>

(i) Soft particles are radiated from the hard particles, and a new population around small momentum is created. They eventually fall into a thermal-like distribution below a scale  $p_{\text{max}}$  :

$$f_{\text{soft}}(p) \sim T_*/p; \quad \text{for } p < p_{\text{max}}. \quad (\text{A.4})$$

(ii) Then, the typical scale  $p_{\text{max}}$  evolves towards UV regime. The evolution of  $p_{\text{max}}$  is dominated by the elastic scattering with the hard particles. When  $p_{\text{max}}$  reaches  $T_*$ , the distribution function becomes comparable to order 1, and then the soft sector is partially thermalized. This time scale can be evaluated as

$$t \sim \alpha^{-5/2} Q^{-1}. \quad (\text{A.5})$$

At this stage, the soft sector dominates the screening effect, the number density and the elastic scattering. However, the energy density is still dominated by the remaining hard particles.

(iii) Finally, the remaining hard particles lose their energies to the soft “thermal” sector by multiple splittings of daughter particles. The system thermalizes when this process is completed. The time scale can be estimated as

$$t_{\text{eq}} \sim (\alpha^2 T_f)^{-1} \sqrt{Q/T_f} \sim \alpha^{-41/16} Q^{-1}. \quad (\text{A.6})$$

---

<sup>#10</sup> In the following, we will only consider gauge bosons since they dominate the equilibration because of the induced emission factor.



Therefore, the equilibration time scale is determined by the time scale for the hard particle  $Q \gg T_f$  to lose its energy in the presence of thermal bath with temperature  $T_f$ .

If the equilibration time scale  $t_{\text{eq}}$ , given by Eq. (A.6), is much smaller than the oscillation time scale  $m_\phi^{-1}$ , we can safely assume that the produced light particles have enough time to thermalize. This condition is given by<sup>#11</sup>

$$1 \ll \alpha^{33/16} \sqrt{\lambda \tilde{\phi}/m_\phi}. \quad (\text{A.8})$$

## B Dissipation coefficient

In this section, we summarize the dissipation coefficient for the sake of completeness.

### B.1 Definition of effective dissipation coefficient

The equation of motion for scalar field is given by

$$\ddot{\phi} + (3H + \Gamma_\phi)\dot{\phi} + m_\phi^2\phi = 0 \quad (\text{B.1})$$

Here  $\Gamma_\phi$  is an amplitude dependent dissipation coefficient. We want to calculate averaged quantities with a time-interval that is longer than the oscillation period but shorter than the Hubble time scale and dissipation time scale. In the following, this time-average is represented by  $\overline{\dots}$ . The energy density of  $\phi$  field is defined by

$$\rho_\phi := \overline{\frac{1}{2}\dot{\phi}^2 + \frac{1}{2}m_\phi^2\phi^2} \quad (\text{B.2})$$

$$= \frac{1}{2}m_\phi^2\tilde{\phi}^2. \quad (\text{B.3})$$

Here  $\tilde{\phi}$  represents an amplitude of  $\phi$ . Using the virial theorem, one can derive the evolution equation for the energy density:

$$\dot{\rho}_\phi + 3H\rho_\phi = -\Gamma_\phi^{\text{eff}}\dot{\rho}_\phi \quad (\text{B.4})$$

where the effective dissipation coefficient is defined as

$$\Gamma_\phi^{\text{eff}} := \frac{\overline{\Gamma_\phi\dot{\phi}^2}}{\dot{\phi}^2}. \quad (\text{B.5})$$

In general, the dissipation coefficient  $\Gamma_\phi$  depends on  $\phi$ , and hence the effective dissipation coefficient  $\Gamma_\phi^{\text{eff}}$  has a non-trivial  $\tilde{\phi}$  ( $\rho_\phi$ ) dependence.

---

<sup>#11</sup> If we keep the mixing angle  $\theta$ , this condition becomes

$$1 \ll \theta^{1/8} \alpha^{33/16} \sqrt{\lambda \tilde{\phi}/m_\phi}. \quad (\text{A.7})$$

## B.2 List of Dissipation Coefficient

Let us summarize the effective dissipation coefficient  $\Gamma_\phi^{\text{eff}}$  as a function of  $\tilde{\phi}$  and  $m_\phi$ .<sup>#12</sup>

(i)  $\lambda\tilde{\phi} \ll m_{\text{th}}^\chi \sim gT$ : In this case, the effective dissipation coefficient is independent of  $\tilde{\phi}$ . Therefore, it is exactly the same as the dissipation coefficient  $\Gamma_\phi$ :

$$\Gamma_\phi^{\text{eff}} = \Gamma_\phi = \dim(r) \begin{cases} \frac{\lambda^2 \alpha T}{2\pi^2} \left[ A_0 + A_1 \left( \frac{m_\phi}{\alpha T} \right)^2 \right] & \text{for } m_\phi < 2m_\chi^{\text{th}}(T) \\ \frac{\lambda^2 m_\phi}{8\pi} \sqrt{1 - 4 \frac{m_{\text{th}}^{\chi^2}}{m_\phi^2} [1 - 2f_{\text{FD}}(m_\phi/2)]} & \text{for } 2m_\chi^{\text{th}}(T) < m_\phi. \end{cases} \quad (\text{B.6})$$

$A_0$  and  $A_1$  are numerical constants, and they are given by  $A_0 \simeq 0.3$  and  $A_1 \simeq 2 \times 10^{-4}$  in our numerical calculation with  $\alpha = 0.05$ . Note that we neglect the hole contribution for simplicity [26].

(ii)  $\lambda\tilde{\phi} \gg m_{\text{th}}^\chi \sim gT$  and  $m_\phi \ll \alpha T$ : In this case, the dissipation coefficient  $\Gamma_\phi$  relevant to the following calculation is given by [10]

$$\Gamma_\phi = \begin{cases} A_0 \dim(r) \frac{\lambda^2 \alpha T}{2\pi^2} & \text{for } \lambda\phi \ll m_{\text{th}}^\chi \\ A_0 \dim(r) \frac{\lambda^4 \phi^2}{\pi^2 \alpha T} & \text{for } m_{\text{th}}^\chi \ll \lambda\phi \ll T \\ \frac{b \alpha^2 T^3}{\phi^2} & \text{for } T \ll \lambda\phi \end{cases} \quad (\text{B.7})$$

where

$$b := \left( \frac{T(r)}{16\pi^2} \right)^2 \frac{(12\pi)^2}{\ln \alpha^{-1}}, \quad (\text{B.8})$$

where  $\dim(r)$  is the dimension of  $\chi$ 's representation  $r$  of gauge group and  $T(r)$  is the index of  $\chi$ 's representation  $r$  that is defined by  $T(r)\delta^{ab} = \text{tr}[t^a(r)t^b(r)]$ . Note that the above dissipation coefficients are computed with two limits; small and large amplitude. Hence we have some ambiguities in the intermediate regime. Using these equations, one can

---

<sup>#12</sup> In what follows, we consider the case where the interaction time scale in thermal plasma is much faster than the dissipation coefficient of inflaton:  $\alpha T \gg \Gamma_\phi$ .

compute the effective dissipation coefficient and it is given by

$$\Gamma_{\phi}^{\text{eff}} = A_0 \dim(r) \frac{\lambda^2 \alpha T}{2\pi^2} \left[ \frac{x}{\pi/2} + \frac{\sin 2x}{\pi} \right] \quad (\text{B.9})$$

$$+ \tilde{A}_0 \dim(r) \frac{\lambda^4 \tilde{\phi}^2}{4\pi^2 \alpha T} \left[ \frac{y'}{\pi/2} - \frac{\sin 4y'}{2\pi} - \frac{x'}{\pi/2} + \frac{\sin 4x'}{2\pi} \right] \quad (\text{B.10})$$

$$+ \frac{b\alpha^2 T^3}{\tilde{\phi}^2} \left[ \frac{4y}{\pi} - 2 + \frac{4}{\pi \tan y} \right] \quad (\text{B.11})$$

where  $x$  and  $y$  are determined case by case as follows.  $\tilde{A}_0$  is a numerical constant and it is given by  $\tilde{A}_0 \simeq 0.2$  for our numerical computation with  $\alpha = 0.05$ .

(ii-i)  $\lambda\tilde{\phi} < g^2 T^2 / m_{\phi}$ : In this case, the non-perturbative production does not occur, and hence  $x$ ,  $x'$ ,  $y'$  and  $y$  are given by

$$x = x' = \begin{cases} \arcsin \frac{m_{\text{th}}^{\chi}}{\lambda\tilde{\phi}} & \text{for } m_{\text{th}}^{\chi} < \lambda\tilde{\phi} \\ \frac{\pi}{2} & \text{for } m_{\text{th}}^{\chi} > \lambda\tilde{\phi} \end{cases} \quad (\text{B.12})$$

$$y = y' = \begin{cases} \arcsin \frac{T}{\lambda\tilde{\phi}} & \text{for } T < \lambda\tilde{\phi} \\ \frac{\pi}{2} & \text{for } T > \lambda\tilde{\phi}, \end{cases} \quad (\text{B.13})$$

It is instructive to study the asymptotic behavior of  $\Gamma_{\phi}^{\text{eff}}$  in two cases: (a)  $\lambda\tilde{\phi} \gg T$  and (b)  $m_{\text{th}}^{\chi} \ll \lambda\tilde{\phi} \ll T$ . In the case of (a),  $x = x'$  and  $y = y'$  are given by

$$x = x' \simeq \frac{m_{\text{th}}^{\chi}}{\lambda\tilde{\phi}} \ll 1, \quad (\text{B.14})$$

$$y = y' \simeq \frac{T}{\lambda\tilde{\phi}} \ll 1. \quad (\text{B.15})$$

Therefore, the effective dissipation coefficient can be approximated by

$$\Gamma_{\phi}^{\text{eff}} \simeq \frac{4}{3\pi^3} \tilde{A}_0 \dim(r) \frac{\lambda T^2}{\alpha \tilde{\phi}} \quad \text{for } \lambda\tilde{\phi} \gg T. \quad (\text{B.16})$$

On the other hand, in the case of (b),  $x = x'$  and  $y = y'$  are given by

$$x = x' \simeq \frac{m_{\text{th}}^{\chi}}{\lambda\tilde{\phi}} \ll 1 \quad (\text{B.17})$$

$$y = y' = \frac{\pi}{2}. \quad (\text{B.18})$$

Then, the dominant contribution to dissipative coefficient can be expressed as

$$\Gamma_{\phi}^{\text{eff}} \simeq \tilde{A}_0 \dim(r) \frac{\lambda^4 \tilde{\phi}^2}{4\pi^2 \alpha T}. \quad (\text{B.19})$$

(ii-ii)  $\lambda\tilde{\phi} > g^2 T^2 / m_{\phi}$ : In this case, the non-perturbative production occurs. Inside the region  $|\phi| < (m_{\phi} \tilde{\phi} / \lambda)^{1/2} =: \phi_{\text{NP}}$ , the adiabaticity is broken down. Hence, we cannot use the WKB solutions inside this region. There are some ambiguities to evaluate the region where the dissipation coefficient is replaced by one caused by the instant preheating, but we simply evaluate the threshold value as  $\phi_{\text{NP}}$ . Then, one can show that the threshold value  $\phi_{\text{NP}}$  is always greater than  $m_{\text{th}}^{\chi}$  from the inequality for non-perturbative production. Therefore, one finds  $x = 0$  and the remaining  $x'$ ,  $y'$  and  $y$  are given by

$$(x', y', y) = \begin{cases} \left( 0, 0, \arcsin \frac{k_*}{\lambda \tilde{\phi}} \right) & \text{for } \phi_{\text{NP}} > T/\lambda \\ \left( \arcsin \frac{k_*}{\lambda \tilde{\phi}}, \arcsin \frac{T}{\lambda \tilde{\phi}}, \arcsin \frac{T}{\lambda \tilde{\phi}} \right) & \text{for } T/\lambda > \phi_{\text{NP}} (> m_{\text{th}}^{\chi} / \lambda). \end{cases} \quad (\text{B.20})$$

(iii)  $\lambda\tilde{\phi} \gg m_{\text{th}}^{\chi} \sim gT$  and  $m_{\phi} > T$ : In this case, the dissipation is dominated by the perturbative decay. Thus, the effective dissipation coefficient is given by

$$\Gamma_{\phi}^{\text{eff}} = \begin{cases} \frac{\lambda^2 m_{\phi}}{8\pi} & \text{for } \lambda\tilde{\phi} \ll m_{\phi} \\ \frac{c\alpha^2 m_{\phi}^3}{\tilde{\phi}^2} \left[ \frac{4y}{\pi} - 2 + \frac{4}{\pi \tan y} \right] & \text{for } \lambda\tilde{\phi} \gg m_{\phi} \end{cases} \quad (\text{B.21})$$

where

$$y = \arcsin \frac{k_*}{\lambda \tilde{\phi}}. \quad (\text{B.22})$$

Here the coefficient  $c$  is given by

$$c = \frac{\dim(\text{Ad})}{4\pi} \left( \frac{T(r)}{4\pi} \right)^2 \quad (\text{B.23})$$

Note that if  $\lambda\tilde{\phi} \gg m_{\phi}$ , the non-perturbative production occurs inevitably.

(iv)  $\lambda\tilde{\phi} > m_{\text{th}}^{\chi} \sim gT$  and  $\alpha T < m_{\phi} < T$ : This is the missed region of our calculation. We simply extrapolate between (ii) and (iii) as a rough approximation.

## References

- [1] A. H. Guth, Phys. Rev. D **23**, 347-356 (1981); A. A. Starobinsky, Phys. Lett. B **91** (1980) 99; K. Sato, Mon. Not. Roy. Astron. Soc. **195**, 467-479 (1981).
- [2] A. D. Linde, Phys. Lett. B **108** (1982) 389; A. Albrecht and P. J. Steinhardt, Phys. Rev. Lett. **48**, 1220 (1982).
- [3] R. Allahverdi, R. Brandenberger, F. -Y. Cyr-Racine and A. Mazumdar, Ann. Rev. Nucl. Part. Sci. **60**, 27 (2010) [arXiv:1001.2600 [hep-th]].
- [4] L. Kofman, A. D. Linde and A. A. Starobinsky, Phys. Rev. Lett. **73**, 3195 (1994) [hep-th/9405187]; Phys. Rev. D **56**, 3258 (1997) [hep-ph/9704452].
- [5] Y. Shtanov, J. H. Traschen and R. H. Brandenberger, Phys. Rev. D **51**, 5438 (1995) [hep-ph/9407247].
- [6] G. N. Felder, L. Kofman and A. D. Linde, Phys. Rev. D **59**, 123523 (1999) [hep-ph/9812289].
- [7] E. W. Kolb, A. Notari and A. Riotto, Phys. Rev. D **68**, 123505 (2003) [hep-ph/0307241].
- [8] J. 'i. Yokoyama, Phys. Lett. B **635**, 66 (2006) [hep-ph/0510091].
- [9] M. Drewes, arXiv:1012.5380 [hep-th].
- [10] K. Mukaida and K. Nakayama, JCAP **1301**, 017 (2013) [arXiv:1208.3399 [hep-ph]].
- [11] F. L. Bezrukov and M. Shaposhnikov, Phys. Lett. B **659**, 703 (2008) [arXiv:0710.3755 [hep-th]].
- [12] J. Garcia-Bellido, D. G. Figueroa and J. Rubio, Phys. Rev. D **79**, 063531 (2009) [arXiv:0812.4624 [hep-ph]].
- [13] R. Allahverdi, K. Enqvist, J. Garcia-Bellido and A. Mazumdar, Phys. Rev. Lett. **97**, 191304 (2006) [hep-ph/0605035].
- [14] K. Nakayama and F. Takahashi, JCAP **1211**, 007 (2012) [arXiv:1206.3191 [hep-ph]].
- [15] R. Micha and I. I. Tkachev, Phys. Rev. Lett. **90**, 121301 (2003) [hep-ph/0210202]; R. Micha and I. I. Tkachev, Phys. Rev. D **70**, 043538 (2004) [hep-ph/0403101].
- [16] J. Berges, A. Rothkopf and J. Schmidt, Phys. Rev. Lett. **101**, 041603 (2008) [arXiv:0803.0131 [hep-ph]]; J. Berges and D. Sexty, Phys. Rev. D **83**, 085004 (2011) [arXiv:1012.5944 [hep-ph]]; J. Berges and D. Sexty, Phys. Rev. Lett. **108**, 161601 (2012) [arXiv:1201.0687 [hep-ph]].

- [17] R. Allahverdi, A. Ferrantelli, J. Garcia-Bellido and A. Mazumdar, Phys. Rev. D **83**, 123507 (2011) [arXiv:1103.2123 [hep-ph]].
- [18] A. Kurkela and G. D. Moore, JHEP **1112**, 044 (2011) [arXiv:1107.5050 [hep-ph]].
- [19] A. Berera, Phys. Rev. Lett. **75**, 3218 (1995) [astro-ph/9509049]; A. Berera, I. G. Moss and R. O. Ramos, Rept. Prog. Phys. **72**, 026901 (2009) [arXiv:0808.1855 [hep-ph]]; M. Bastero-Gil and A. Berera, Int. J. Mod. Phys. A **24**, 2207 (2009) [arXiv:0902.0521 [hep-ph]].
- [20] M. Bastero-Gil, A. Berera and R. O. Ramos, JCAP **1109**, 033 (2011) [arXiv:1008.1929 [hep-ph]].
- [21] M. B. Einhorn and D. R. T. Jones, JHEP **1003**, 026 (2010) [arXiv:0912.2718 [hep-ph]]; S. Ferrara, R. Kallosh, A. Linde, A. Marrani and A. Van Proeyen, Phys. Rev. D **82**, 045003 (2010) [arXiv:1004.0712 [hep-th]]; Phys. Rev. D **83**, 025008 (2011) [arXiv:1008.2942 [hep-th]]; H. M. Lee, JCAP **1008**, 003 (2010) [arXiv:1005.2735 [hep-ph]].
- [22] K. Nakayama and F. Takahashi, JCAP **1102**, 010 (2011) [arXiv:1008.4457 [hep-ph]].
- [23] M. Hindmarsh and D. R. T. Jones, arXiv:1203.6838 [hep-ph].
- [24] A. D. Linde, Phys. Lett. B **259**, 38 (1991); Phys. Rev. D **49**, 748 (1994) [astro-ph/9307002].
- [25] E. J. Copeland, A. R. Liddle, D. H. Lyth, E. D. Stewart and D. Wands, Phys. Rev. D **49**, 6410 (1994) [astro-ph/9401011]; G. R. Dvali, Q. Shafi and R. K. Schaefer, Phys. Rev. Lett. **73**, 1886 (1994) [hep-ph/9406319].
- [26] M. Le Bellac, “Thermal Field Theory,” Cambridge University Press, Cambridge, UK (2000).